Proceedings of the 25th Annual International Conference of the IEEE EMBS
Cancun, Mexico • September 17-21, 2003

Principal Dynamic Mode Analysis of a Spider Mechanoreceptor Action Potentials

Georgios D. Mitsis[1], Spiros Courellis[1], Andrew S. French[2] and Vasilis Z. Marmarelis[1]
[1] Department of Biomedical Engineering, University of Southern California, Los Angeles CA, USA
[2] Department of Physiology and Biophysics, Dalhousie University, Halifax, Canada

Abstract – **The nonlinear dynamics of a spider mechanoreceptor are examined using the Principal Dynamic Mode (PDM) methodology. The cuticilar sense organ of an adult *Cupiennius Salei* spider was stimulated with a pseudorandom Gaussian process spectrally bound at 400 Hz and the resulting action potentials were recorded. Data analysis reveals three PDMs that describe the system dynamics, based on the second order Volterra kernel, which is estimated from the recorded input/output datasets. The first PDM exhibits high-pass behavior, illustrating the importance of the speed of the slit displacement to the mechanoreceptor, while the other two PDMs exhibit bandpass behavior. The probability of firing an action potential is represented by a static multiple-input nonlinearity that receives the values of the convolution of each mode with the pseudorandom input as its inputs. The probability of firing function exhibits asymmetric behavior with respect to its arguments, suggesting directional dependence of the mechanoreceptor response on the PDM outputs. Trigger regions for a probability threshold value of 0.1 are also presented.**

Keywords – **Action potentials, Laguerre expansion, Mechanoreceptors, Nonlinear modeling, Volterra kernels.**

I. Introduction

Mechanoreceptors perform the transduction and detection of mechanical stimuli for both sensory and regulatory purposes. They should operate with sufficient sensitivity in order to detect small stimuli and at the same time accommodate naturally occurring stimuli over a wide operating range. The dynamic behavior of mechanoreceptors and their underlying molecular mechanisms are not yet well understood, mainly because of the small size and inaccessibility of most mechanoreceptors.

In this paper, the principal dynamic mode (PDM) methodology [1] is employed in order to study the action potential firing in a spider mechanoreceptor in response to pseudorandom mechanical stimuli. Specifically, single neurons of a slit-sense organ in the spider, *Cupiennius salei,* were stimulated with pseudorandom broadband displacements and the generated action potentials were measured. These data are used to obtain Volterra kernel estimates and the equivalent PDM model.

The interpretation of the resulting dynamic model is discussed and indicates the presence of three distinct biophysical mechanisms (one high-pass and two band-pass), corresponding to the three PDMs of this system. These results are consistent with a previously published modeling study on intracellular data from this system [2].

II. Methodology

Experimental methods

The mechanical stimulus was applied by compressing the cuticular slits of a cuticular sense organ, taken from the leg of adult *Cupiennius salei* spiders. In this way the sensory endings of the bipolar mechanoreceptor endings were subjected to mechanical displacement. The stimulus delivered was pseudorandomly modulated with a Gaussian amplitude distribution and spectrally flat up to 400 Hz. The sampling frequency of the stimulus and the action potential responses was 1 KHz.

Mathematical methods

The first and second-order Volterra kernels of the system were obtained by employing the Laguerre expansion technique [3] for the mechanical forcing input and action potential output. The Volterra kernels were consequently employed to compute the PDMs of the system. Based on the magnitude of the eigenvalues of the matrix constructed by the Volterra kernels [1], it was determined that three modes are sufficient to describe the system.

The representation of the nonlinear dynamic behavior of the mechanoreceptor is shown in Fig. 1. The outputs of the three PDMs $\{\mu_i\}$ are given by their convolution with the input signal:

$$u_i(n) = \sum_{m=0}^{M_i} \mu_i(m)\, x(n-m) \qquad i=1,2,3 \quad (1)$$

and are combined into a multiple-input nonlinearity $f(u_1,u_2,u_3)$, which is defined as the locus of points $\{u_1,u_2,u_3\}$ that correspond to an output action potential [4].

The output of the model is finally given by comparing the output of $f(u_1,u_2,u_3)$ with a threshold p:

$$\hat{y}(n) = \begin{cases} 1 & \text{if } f[u_1(n),u_2(n),u_3(n)] - p > 0 \\ 0 & \text{if } f[u_1(n),u_2(n),u_3(n)] - p \le 0 \end{cases} \quad (2)$$

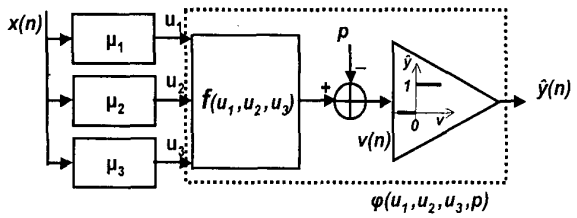

Figure 1. Principal dynamic mode representation of action potential firing in a spider mechanoreceptor. The input signal (mechanical displacement) is fed into the linear modes of the system, which are combined by a multiple-input threshold to produce action potentials.

III. RESULTS

The obtained first-order Volterra kernels for a representative data set are given in Fig. 2 in the time and frequency domains. The corresponding second-order kernel is shown in Fig. 3. Both exhibit a memory of around 10 msec. The main peak of the first-order kernel resides at around 180 Hz, while the second-order kernel exhibits high-pass characteristics.

The three PDMs are shown in Fig. 4 in the time and frequency domains. In this case, the magnitudes of the corresponding eigenvalues are equal to 2.28, 0.31 and 0.22 for modes 1, 2 and 3 respectively and indicate the relative contribution of the three significant modes on the output. The first mode exhibits clearly a high-pass characteristic, whereas the other two modes exhibit bandpass characteristics with main peaks at 120 Hz and 180 Hz for modes 2 and 3 respectively.

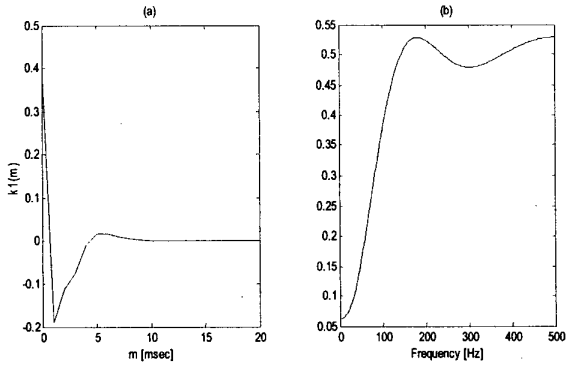

Figure 2. First-order Volterra kernel (a)Time domain (b)Frequency domain

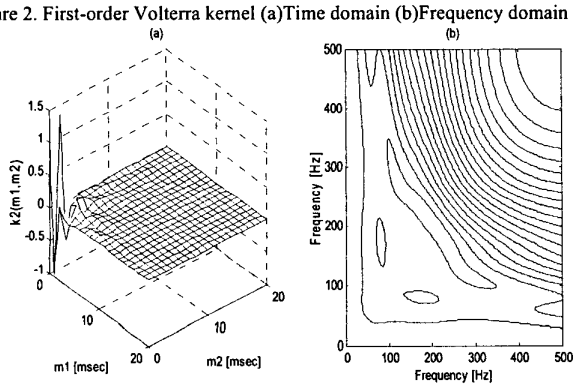

Figure 3. Second-order Volterra kernels (a)Time domain (b)Frequency domain.

The nonlinearity $f(u_1,u_2,u_3)$ is computed as described in the Methodology section. The probability of action potential firing is determined by dividing the range of values of the mode outputs into bins of appropriate size, counting the total number of $\{u_1,u_2,u_3\}$ values that give rise to action potential firing within each bin and normalizing by the total number of $\{u_1,u_2,u_3\}$ values in the same bin (by taking also into consideration the refractory period for action potential generation). The obtained probability functions as a function of the three possible different $\{u_1,u_2,u_3\}$ pairs (i.e., by "projecting" onto the corresponding plane) are shown in Figs. 5-7. All three demonstrate a ramp-threshold characteristic. The probability as a function of $\{u_1,u_2\}$ is almost zero for positive values of u_2, whereas for negative values of the latter it increases with increasing positive values of u_1. The probability as a function of $\{u_1,u_3\}$ is more dependent on the values of u_1, increasing sharply with larger positive values of the latter, both for positive and negative u_3 values. However, it can be observed that for negative values of u_1, it is nonzero only for negative values of u_3. The third probability function is nonzero for negative values of u_2, u_3 (as can be inferred by the form of the rest of the projection) and increases markedly for increasingly negative values of u_2.

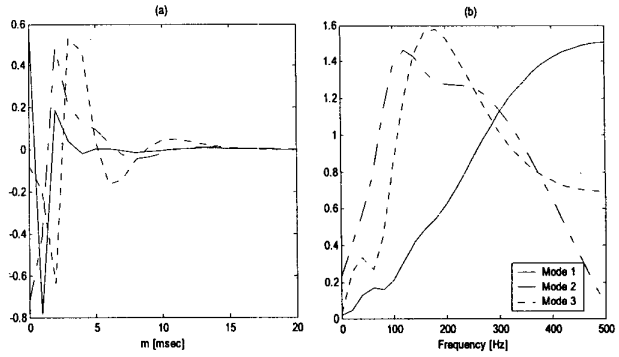

Figure 4. Estimated principal dynamic modes (a) Time domain (b) Frequency domain.

Finally, the trigger regions resulting by applying a threshold p equal to 0.1 to the probability functions of Figs. 5-7 are plotted in Figs. 8-10 and illustrate the above observations more clearly.

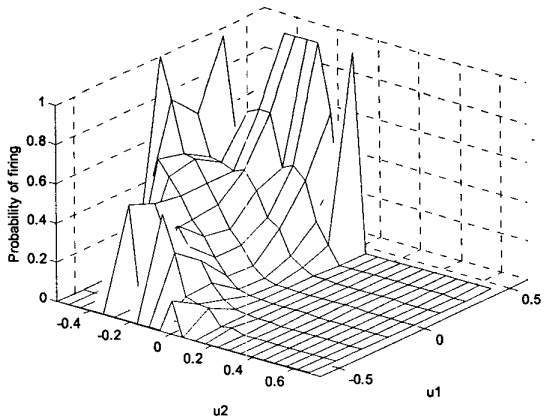

Figure 5. Probability of firing an action potential as a function of the outputs of modes 1 and 2.

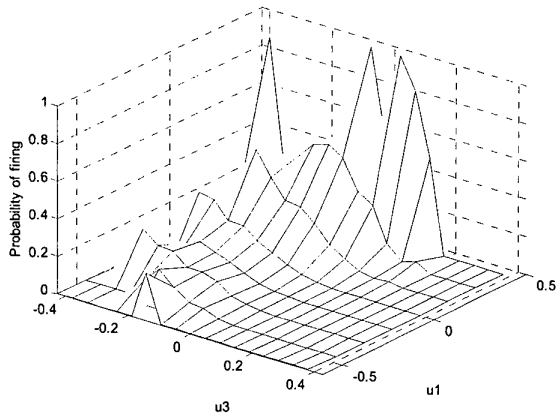

Figure 6. Probability of firing an action potential as a function of the outputs of modes 1 and 3.

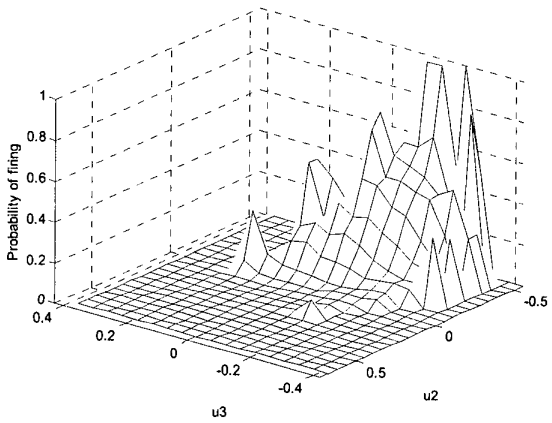

Figure 7. Probability of firing an action potential as a function of the outputs of modes 2 and 3.

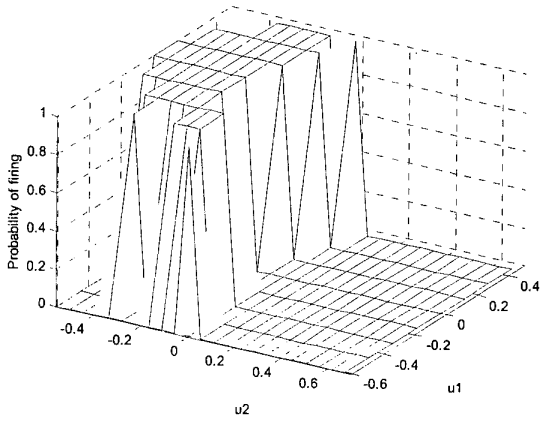

Figure 8. Trigger region as a function of u_1, u_2 for a threshold of 0.1.

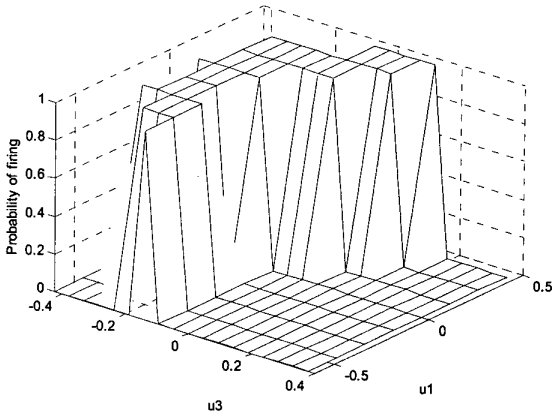

Figure 9. Trigger region as a function of u_1, u_3 for a threshold of 0.1.

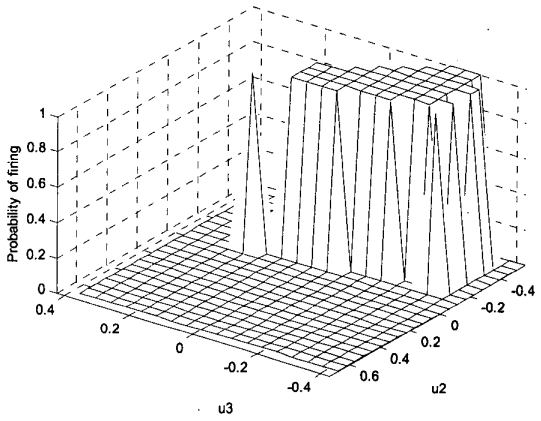

Figure 10. Trigger region as a function of u_2, u_3 for a threshold of 0.1.

IV. Discussion

The three PDMs that describe the spider mechanoreceptor dynamics correspond to the most significant dynamic components responsible for the mechanoreceptor's response to a pseudorandom Gaussian input. Moreover, they divide the frequency response characteristic of the mechanoreceptor in three regions. The first mode dominates for frequencies above 300 Hz, while the other two dominate for frequencies below 300 Hz.

The first and most significant computed PDM exhibits a strongly high-pass characteristic. Its differentiating properties suggest that one of the input attributes that the mechanoreceptor responds to is the speed of the slit displacement. The mode is mainly residing in the second-order kernel, implying that the speed of the slit displacement affects the response of the system mainly through nonlinear mechanisms.

Modes 2 and 3 exhibit a band-pass characteristic and most of their power lies in the low frequency range. They are mostly responsible for processing the amplitude of the displacement of the slit rather than its speed. Of all three modes, mode 3 resembles the first-order kernel.

The firing probability function $f(u_1, u_2, u_3)$ exhibits (directional) ramp-threshold behavior with respect to its arguments. Its projection on the (u_1, u_2) plane (Fig. 5) indicates that mode 2 is influencing firing considerably more than mode 1. Values of u_2 less than zero are mainly responsible for firing, while values of u_2 greater than zero inhibit firing. Moreover, the probability of firing increases for decreasing values of u_2 and increasing values of u_1. This behavior reveals an asymmetry of the firing probability function with respect to u_1 and u_2. This asymmetry emphasizes one mode (in this case u_2) in deciding whether to fire or not.

Similar observations can be made for the projections of the firing probability function in (u_1, u_3) and (u_1, u_3). The (u_1, u_3) projection (Fig. 6) displays ramp-threshold in the direction of u_1 emphasizing mode 1 as the decisive mode for firing, assisted by decreasing negative values of u_3. The (u_2, u_3) projection (Fig. 7) displays ramp-threshold in the direction of u_2 emphasizing mode 2 as the decisive mode for firing, assisted by decreasing negative values of u_3. Asymmetry is present in these projections as well.

V. Conclusion

The preliminary results presented in this paper demonstrate the ability of the PDM methodology to capture the dynamic characteristics of the spider mechanoreceptor associated with the amplitude and the speed of the slit displacement. They also illustrate a method to define a firing probability function that combines the values of the convolution of each mode with the input and specify trigger regions based on it. The PDMs and the firing probability function offer a simplified model that could potentially describe the behavior not only of the spider mechanoreceptor, but mechanoreceptors in other species too. In order to properly evaluate the obtained PDM model that employs the probability of firing function, the notion of a "sensitivity-specificity curve" (SSC) (akin to the receiver operating characteristic in detection problems) must be utilized. The SSC provides the relation between the probability of predicting an output spike correctly (sensitivity) versus the probability of a false prediction (one minus specificity) for each selected output threshold. The performance of the model is deemed better when the area under the SSC is greater.

References

[1] V.Z. Marmarelis "Modeling methodology for nonlinear physiological systems," *Ann. Biomed. Eng.* 25:239-251, 1997.

[2] V.Z. Marmarelis, M. Juusola and A.S. French "Principal dynamic mode analysis of nonlinear transduction in a spider mechanoreceptor," *Ann. Biomed. Eng.* 27: 391-402, 1999.

[3] V.Z. Marmarelis "Identification of nonlinear biological systems using Laguerre expansion of kernels," *Ann. Biomed. Eng.* 21: 573-589, 1993.

[4] V.Z Marmarelis "Signal transformation and coding in neural systems," *IEEE Trans. Biomed. Engin.* 36:15-24, 1989.